VIP Protein–Protein Interactions

DOI: 10.1002/anie.200907203

Identification and Structure of Small-Molecule Stabilizers of 14–3–3 Protein–Protein Interactions**

*Rolf Rose, Silke Erdmann, Stefanie Bovens, Alexander Wolf, Micheline Rose, Sven Hennig, Herbert Waldmann, and Christian Ottmann**

Inhibition of protein–protein interactions (PPIs) with small molecules has gained substantial interest in pharmaceutical research and provided novel opportunities for the treatment of disease.[1–5] However, the alternative development of small molecules that stabilize protein–protein interactions has been achieved in only very few cases,[6,7] typically including structurally complex natural products that are usually produced by fermentation and isolation from natural sources.[8–11] These compounds are however widely employed in basic research and even in clinical use, thereby demonstrating the value of this approach. Therefore, the identification and development of small-molecule PPI stabilizers that are tractable by organic synthesis and can be optimized in terms of potency and specificity is of major interest.

A particularly relevant case is given by the 14–3–3 proteins and their interaction with target proteins. The 14–3–3 proteins are a highly conserved class of adapter proteins that are involved in the regulation of several hundred proteins, among them important pharmaceutical targets such as Raf, p53, Cdc25, Cdk2, and histone deacetylases (HDACs).[12] Binding of 14–3–3 proteins can either be inhibitory, such as in the case of the Cdc25 phosphatases,[13] or it can be stimulatory as in the case of the tumor suppressor protein p53.[14] Depending on the physiological context, for example in different cancers, the stabilization of a regulatory 14–3–3 protein–protein complex might be of therapeutic value. However, small molecule stabilizers of these therapeutically interesting interactions are not known. An example of a natural 14–3–3 PPI-stabilizing small molecule is the specific 14–3–3 protein–protein interaction with the plant proton pump PMA2, which can be stabilized by the fungal toxin fusicoccin.[15] This natural compound binds to a site preformed by the two proteins and mediates its stabilizing function by simultaneously contacting both partner proteins.[16,17]

Herein we report on the identification of two small molecules that selectively stabilize the 14–3–3/PMA2 protein–protein interaction by binding to two adjacent sites in the interface, and which are active in vivo. To identify potential stabilizing molecules, we screened a 37000-member compound library in a surface-based format monitoring the binding of green fluorescent protein (GFP) fused with 14–3–3 to surface-immobilized gluthatione S-transferase (GST) fused with PMA2-CT52 (the C-terminal 52 amino acids of PMA2; see the Supporting Information). The initial screen successfully identified two structurally unrelated compounds with the desired activity (Figure 1a). For these compounds, the kinetics of the stabilizing activity were determined by means of surface plasmon resonance (SPR; Figure 1b). To this end, the 14–3–3 interaction domain of PMA2, that is, the 52 C-terminal amino acids (CT52)[17] was immobilized on the dextran matrix of a BiaCore chip, and binding of the 14–3–3 protein was measured in the presence of the protein-protein interaction-stabilizing small molecule. The trisubstituted pyrrolinone hit compound, pyrrolidone1, showed association kinetics similar to fusicoccin (Figure 1b) but with a more rapid dissociation, resulting in a K_D of 80 μM. The dipeptide epibestatin displayed a different kinetic behavior in stabilizing the 14–3–3/PMA2 complex, with a slower association than fusicoccin and pyrrolidone1 (Figure 2b). However, the dissociation kinetics of epibestatin resembled that of fusicoccin; that is, the protein complex was very stable once it was constituted and dissociation was very slow. As a result, the calculated K_D of the 14–3–3/PMA2 complex in the presence of epibestatin was 1.8 μM. In the absence of any stabilizing compound no binding of 14–3–3 to immobilized PMA2 could be measured (Figure 1b, DMSO control).

To unravel the mechanistic basis of the obviously different binding modes of pyrrolidone1 and epibestatin, the crystal structures the ternary complexes with 14–3–3 and the C-terminal 30 amino acids of PMA2 (PMA2-CT30) were solved. We obtained co-crystals by mixing 14–3–3 protein and PMA2-CT30 (1:1.5 ratio) in the presence of either 2 mM pyrrolidone1 or 2 mM epibestatin. Both protein complexes crystallized in

[*] Dr. R. Rose, Dr. S. Erdmann, Dr. S. Bovens, Dr. A. Wolf, M. Rose, Dr. S. Hennig, Dr. C. Ottmann
Chemical Genomics Centre of the Max Planck Society
Otto-Hahn-Strasse 15, 44227 Dortmund (Germany)
Fax: (+49) 231-133-2499
E-mail: christian.ottmann@cgc.mpg.de
Homepage: http://www.cgc.mpg.de
Prof. Dr. H. Waldmann
Max-Planck-Institut für molekulare Physiologie
Abteilung Chemische Biologie
Otto-Hahn-Strasse 11, 44227 Dortmund (Germany)
and
Technische Universität Dortmund, Fakultät Chemie
Lehrbereich Chemische Biologie
Otto-Hahn-Strasse 6, 44227 Dortmund (Germany)

[**] This work was supported by the Max Planck Society and BMBF grant GO-Bio 0313873 (to R.R., S.B., S.E., A.W., M.R., and S.H.). We thank Alfred Wittinghofer for helpful discussions and the staff at the Swiss Light Source, beamline X10SA, for support during crystallographic data collection. The atomic coordinates and structure factors of the T14-3e/CT30/pyrrolidone1 and the T14-3e/CT30/epibestatin complex have been deposited in the Protein Data Bank (PDB) under the ID codes 3M51 and 3M50.

Supporting information for this article is available on the WWW under http://dx.doi.org/10.1002/anie.200907203.

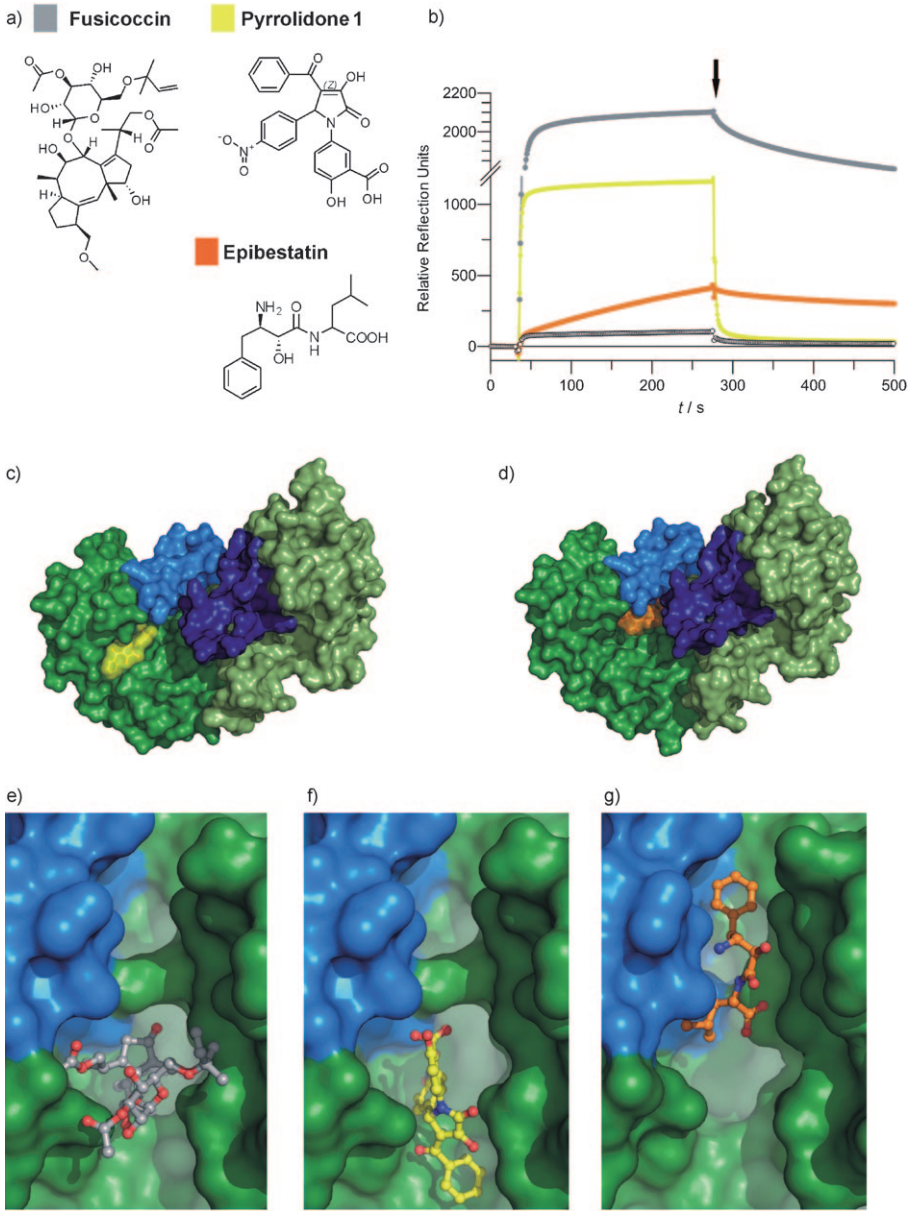

Figure 1. Pyrrolidone1 and epibestatin stabilize the 14–3–3/PMA2 complex in different ways to each other and to fusicoccin. a) Structures of fusicoccin, pyrrolidone1, and epibestatin. b) The association/dissociation of 14–3–3 to the binding domain of PMA2 (CT52) was measured with surface plasmon resonance (BiaCore) in the presence of fusicoccin (5 μM, gray) pyrrolidone1 (50 μM, yellow), and epibestatin (50 μM, orange) or in DMSO as control (open). The turning point from the association to the dissociation phase of the experiment is indicated. c) Crystal structure of pyrrolidone1 (yellow) bound to the binary complex of 14–3–3 (green) and PMA2-CT30 (blue surface). d) Epibestatin (orange) bound to the 14–3–3/PMA2-CT30 complex. e) Superimposition of fusicoccin (gray) bound to the 14–3–3/PMA2-CT30 (surface representation, color coding as in (c) and derived from our previously published 14–3–3/PMA2-CT52 complex structure (PDB code: 2O98).[17] f) Binding site of pyrrolidone1 (yellow) in the 14–3–3/PMA2-CT30 complex. g) Binding site of epibestatin (orange) in the 14–3–3/PMA2-CT30 complex.

the same space group, but whilst the epibestatin crystals diffracted reproducibly to 2.6 Å, the crystals of the pyrrolidone1 complex did not diffract beyond 3.2 Å. Nevertheless, we were able to determine the binding and orientation at the interface of the two protein partners for both molecules (Figure 2e,f; Supporting Information, Figure S1,S2).

The different association/dissociation kinetics of pyrrolidone1 and epibestatin are reflected in their binding modes. Pyrrolidone1 shares most of its protein contact surface with 14–3–3 (288.2 Å^2 from a total of 349.7 Å^2; 83%) and binds to a site that is highly accessible from the solvent space, which might contribute to its fast association kinetics (Figure 1b,c). The contacts to PMA2 are rather limited (Figure 1f, Figure 2a), a fact that together with the general exposed character of its binding pocket might account for the high dissociation rate of the complex. In contrast to pyrrolidone1, epibestatin is more deeply buried in the protein complex and is literally trapped between 14–3–3 and PMA2 (Figure 1d), and shares a roughly equal contact surface with 14–3–3 (164.4 Å^2, 55%) and PMA2 (135.5 Å^2, 45%; Figure 1g). These characteristics are in accordance with the observed slow association and dissociation kinetics.

Pyrrolidone1 shares part of its binding site with fusicoccin (Figure 2a) but is coordinated in quite a different way. Fusicoccin almost completely fills the cavity of the binding groove of 14–3–3, whereas pyrrolidone1 only partially fills this region (Figure 2a–c). This binding mode indicates that appropriate variation of the structure of this inhibitor type may yield compounds that completely fill the gap in the interface of the two proteins. Epibestatin, like fusicoccin, fills its binding site, a crevice between the two proteins, to a considerably higher extent than observed for pyrrolidone1 (Figure 2d). Therefore, the binding mode of epibestatin suggests a strong shape-driven component that is comparable to the binding mode of fusicoccin. The more intimate contact to both protein partners probably accounts for the stronger potency of epibestatin in stabilizing the 14–3–3/PMA2 complex. Details of the protein contacts of both compounds are shown in Figure 2e and f.

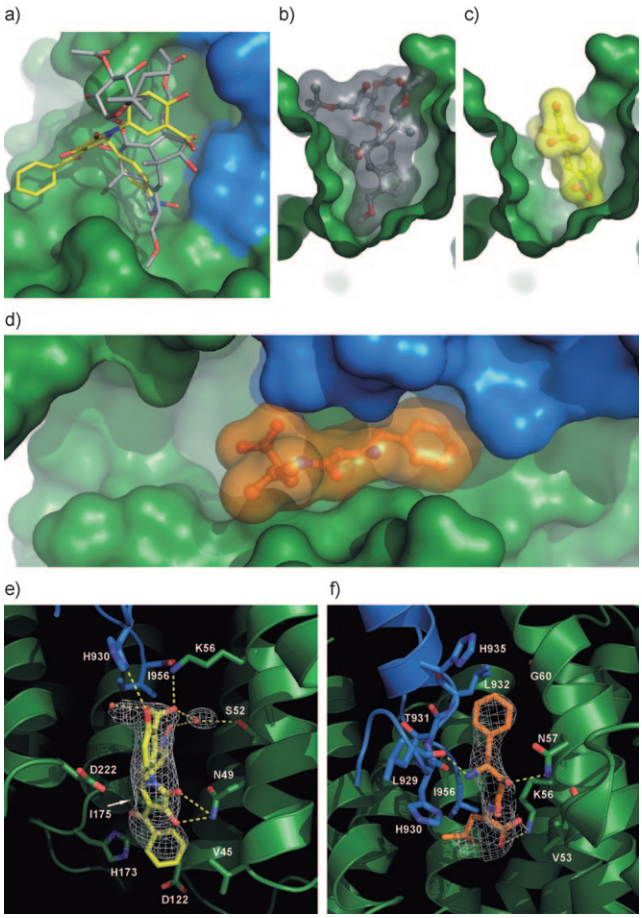

Figure 2. Comparison of the binding modes of fusicoccin, pyrrolidone1, and epibestatin. a) Superimposition of fusicoccin (gray) and pyrrolidone1 (yellow) bound to the 14–3–3/PMA2-CT30 complex (green and blue surface, respectively). b) Fusicoccin (gray) fills the profile of the 14–3–3 binding grove (green) almost completely. c) Pyrrolidone1 (yellow), in contrast to fusicoccin, occupies only about one third of the 14–3–3 binding grove profile. d) Binding of epibestatin (yellow) to a crevice-like site between 14–3–3 (green) and PMA2-CT30 (blue). e) Residues from 14–3–3 (green) and PMA2 (blue) implicated in the coordination of pyrrolidone1 (yellow). Polar contacts are indicated as yellow lines, the $2F_{obs}-F_{calc}$ electron density of pyrrolidone1 (contoured at 1 σ) and two water molecules (red spheres) is shown in white. f) Residues of the 14–3–3/PMA2 complex (color coding as in (e)) implicated in binding of epibestatin (orange) with the the $2F_{obs}-F_{calc}$ electron density of epibestatin (contoured at 1 σ) shown in white.

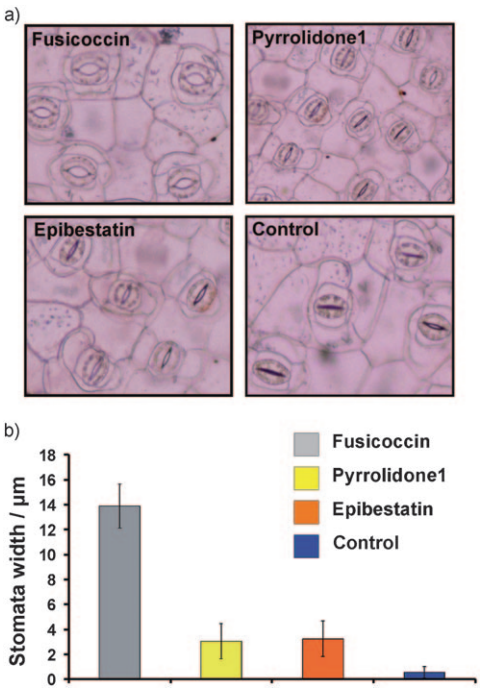

Figure 3. Pyrrolidone1 and epibestatin show fusicoccin-specific activity in plant cells. a) Opening of stomatal pores in the presence of fusicoccin (5 µM), pyrrolidone1 (50 µM), and epibestatin (50 µM). The epidermis of leaves from the Asiatic dayflower (*Commelina communis*) were incubated for 3 h in buffered solutions containing fusicoccin, pyrrolidone1, epibestatin, or DMSO (control) and the opening width were analyzed by light microscopy. b) Median opening width of stomata after 3 h treatments of epidermal preparations from *Commelina communis*.

The stabilization of the 14–3–3/PMA2 complex by fusicoccin leads to activation of the proton pump, opening of the stomata, which are the gas-exchanging pores on the leaf surface, and subsequent wilting of the plant.[18,19] To determine whether the two compounds identified in our biochemical screen also display in vivo activity, we employed a stomata-opening test in which isolated epidermis of leaves from the Asiatic dayflower (*Commelina communis*) is incubated with the test compounds. After three hours, the opening width of the stomatal pores was measured by light microscopy (Figure 3a). In the presence of 50 µM pyrrolidone1 or epibestatin, stomatal pores opened 3 µm and 3.2 µm on average, respectively. This data clearly indicate in vivo potency of pyrrolidone1 and epibestatin as activators of the plant proton pump.

The fact that pyrrolidone1 and epibestatin are chemically unrelated to each other and furthermore show no structural resemblance to fusicoccin is of particular note for the strategy to employ small molecule 14–3–3 protein–protein stabilizers. The initial discovery of different chemotypes from a limited primary screening for a certain 14–3–3 protein–protein interaction indicates that further compound classes may be found. As the actual binding sites of protein–protein stabilizing molecules are constituted by both protein partners, the intrinsic specificity of these molecules may be very high. To investigate this possibility, we tested epibestatin and pyrrolidone1 in regard to their potential ability to stabilize other 14–3–3 protein–protein interactions, including Raf1, p53, Cdc25C, RNF11, Mlf1, AICD, Cby, and YAP (Supporting Information, Figure S3,S4). Both compounds showed no activity in stabilizing the binding of 14–3–3 to any of these targets. Although this investigation is not comprehensive, our data indicate that it might be possible to identify specific small molecules that stabilize distinct 14–3–3 protein–protein

interactions with high selectivity. Such specific molecules would be valuable tools in investigating the biology of 14–3–3 protein–protein interactions with a plethora of target proteins and might be promising starting points for the development of medicinally active agents.

Received: December 21, 2009
Revised: March 1, 2010
Published online: April 30, 2010

Keywords: 14–3–3 proteins · crystal structures · drug discovery · protein–protein interactions · surface plasmon resonance

[1] J. A. Wells, C. L. McClendon, *Nature* **2007**, *450*, 1001 – 1009.
[2] L. T. Vassilev, B. T. Vu, B. Graves, D. Carvajal, F. Podlaski, Z. Filipovic, N. Kong, U. Kammlott, C. Lukacs, C. Klein, N. Fotouhi, E. A. Liu, *Science* **2004**, *303*, 844 – 848.
[3] T. Oltersdorf, S. W. Elmore, A. R. Shoemaker, R. C. Armstrong, D. J. Augeri, B. A. Belli, M. Bruncko, T. L. Deckwerth, J. Dinges, P. J. Hajduk, M. K. Joseph, S. Kitada, S. J. Korsmeyer, A. R. Kunzer, A. Letai, C. Li, M. J. Mitten, D. G. Nettesheim, S.-C. Ng, P. M. Nimmer, J. M. O'Connor, A. Oleksijew, A. M. Petros, J. C. Reed, W. Shen, S. K. Tahir, C. B. Thompson, K. J. Tomaselli, B. Wang, M. D. Wendt, H. Zhang, S. W. Fesik, S. H. Rosenberg, *Nature* **2005**, *435*, 677 – 681.
[4] M. M. He, A. S. Smith, J. D. Oslob, W. M. Flanagan, A. C. Braisted, A. Whitty, M. T. Cancilla, J. Wang, A. A. Lugovskoy, J. C. Yoburn, A. D. Fung, G. Farrington, J. K. Eldredge, E. S. Day, L. A. Cruz, T. G. Cachero, S. K. Miller, J. E. Friedman, I. C. Choong, B. C. Cunningham, *Science* **2005**, *310*, 1022 – 1025.
[5] T. M. Bonacci, J. L. Mathews, C. Yuan, D. M. Lehmann, S. Malik, D. Wu, J. L. Font, J. M. Bidlack, A. V. Smrcka, *Science* **2006**, *312*, 443 – 446.
[6] S. S. Ray, R. J. Nowak, R. H. Brown, Jr., P. T. Lansbury, Jr., *Proc. Natl. Acad. Sci. USA* **2005**, *102*, 3639 – 3644.
[7] P. Hammarström, R. L. Wiseman, E. T. Powers, J. W. Kelly, *Science* **2003**, *299*, 713 – 716.
[8] J. Choi, J. Chen, S. L. Schreiber, J. Clardy, *Science* **1996**, *273*, 239 – 242.
[9] J. P. Griffith, J. L. Kim, E. E. Kim, M. D. Sintchak, J. A. Thomson, M. J. Fitzgibbon, M. A. Fleming, P. R. Caron, K. Hsiao, M. A. Navia, *Cell* **1995**, *82*, 507 – 522.
[10] L. Renault, B. Guibert, J. Cherfils, *Nature* **2003**, *426*, 525 – 530.
[11] J. J. G. Tesmer, R. K. Sunahara, A. G. Gilman, S. R. Sprang, *Science* **1997**, *278*, 1907 – 1916.
[12] H. Hermeking, *Nat. Rev. Cancer* **2003**, *3*, 931 – 943.
[13] C. Y. Peng, P. R. Graves, R. S. Thoma, Z. W. Wu, A. S. Shaw, H. Piwnica-Worms, *Science* **1997**, *277*, 1501 – 1505.
[14] M. J. Waterman, E. S. Stavridi, J. L. Waterman, T. D. Halazonetis, *Nat. Genet.* **1998**, *19*, 175 – 178.
[15] C. Oecking, C. Eckerskorn, E. W. Weiler, *FEBS Lett.* **1994**, *352*, 163 – 166.
[16] M. Würtele, C. Jelich-Ottmann, A. Wittinghofer, C. Oecking, *EMBO J.* **2003**, *22*, 987 – 994.
[17] C. Ottmann, S. Marco, N. Jaspert, C. Marcon, N. Schauer, M. Weyand, C. Vandermeeren, G. Duby, M. Boutry, A. Wittinghofer, J.-L. Rigaud, C. Oecking, *Mol. Cell* **2007**, *25*, 427 – 440.
[18] C. Oecking, M. Piotrowski, J. Hagemeier, K. Hagemann, *Plant J.* **1997**, *12*, 441 – 453.
[19] N. C. Turner, A. Graniti, *Nature* **1969**, *223*, 1070 – 1071.

